Automatic control and tracking of periodic orbits in chaotic systems

Hiroyasu Ando,[1,2] S. Boccaletti,[3,4] and Kazuyuki Aihara[1,2,5]
[1]*Department of Mathematical Informatics, The University of Tokyo, 7-3-1 Hongo, Bunkyo-ku, Tokyo 113-8656, Japan*
[2]*Aihara Complexity Modelling Project, ERATO, JST, 3-23-5 Uehara, Shibuya-ku, Tokyo 151-0064, Japan*
[3]*CNR-Istituto dei Sistemi Complessi, Via Madonna del Piano, 10, 50019 Sesto Fiorentino (FI), Italy*
[4]*Embassy of Italy in Tel Aviv, Trade Tower, 25 Hamered Street, Tel Aviv, Israel*
[5]*Institute of Industrial Science, The University of Tokyo, 4-6-1 Komaba, Meguro-ku, Tokyo 153-8505, Japan*
(Received 6 December 2006; revised manuscript received 28 April 2007; published 20 June 2007)

Based on an automatic feedback adjustment of an additional parameter of a dynamical system, we propose a strategy for controlling periodic orbits of desired periods in chaotic dynamics and tracking them toward the set of unstable periodic orbits embedded within the original chaotic attractor. The method does not require information on the system to be controlled, nor on any reference states for the targets, and it overcomes some of the difficulties encountered by other techniques. Assessments of the method's effectiveness and robustness are given by means of the application of the technique to the stabilization of unstable periodic orbits in both discrete- and continuous-time systems.

DOI: 10.1103/PhysRevE.75.066211 PACS number(s): 05.45.Gg, 05.45.Pq

I. INTRODUCTION

Control of chaos refers to a process wherein a judiciously chosen perturbation is applied to a chaotic system in order to realize desirable (chaotic or periodic) behavior. Since the seminal contribution by Ott, Grebogi, and Yorke (OGY) in 1990 [1], this concept of harnessing chaotic behavior has been variously developed and found a huge number of applications [2].

The two most widely used approaches to realize such a process are the OGY-based techniques and the methods based on time-delayed feedback control (DFC) [3]. While the OGY-based methods stabilize unstable periodic orbits (UPOs) embedded within the chaotic attractor using small time-dependent perturbations of some accessible control parameters, they in general require a reconstruction of the parametrical variations in the UPOs' stable and unstable manifolds in some section of the flow, which might make difficult their real-time experimental applications to fast dynamical systems. On the other hand, the DFC-based methods and their extensions [4–6] use a direct time-delayed feedback on an accessible system's variable. However, they need to tune principal parameters, such as the feedback gain and the delay time, in advance.

In this paper, we devise a technique to control chaotic behavior into a desired periodic one, which is able to overcome both such difficulties. The method adaptively modifies the so-called constant-feedback (CF) method [7], which makes use of an additional parameter to create new dynamics in the original system and stabilizes periodic orbits (POs) in the new dynamics. The CF method, indeed, shares with OGY and DFC methods the great advantage that no *a priori* information on the original system is required and has been widely applied [8,9].

The proposed technique tunes adaptively and automatically the CF's additional parameter, and therefore it has an advantage over the standard CF method in that not even knowledge of the additional bifurcation analysis with respect to the new parameter is required [10]. An adaptive-feedback scheme for control of chaotic systems has gathered attention recently [11,12].

II. CONTROL METHOD

For the sake of exemplification, let us start with illustrating the technique for discrete-time systems. The control process consists of two stages. In the first stage, the CF's parameter is tuned automatically to the value which produces a desired PO. In the second stage, the new dynamics created by the changes in the CF's parameter is tracked back to the original one (by slightly changing the CF's parameter up to vanishing its value) and therefore the controlled POs are included in the set of UPOs embedded within the original chaotic attractor. It is important to emphasize that the vanishing of the control force over the controlled UPOs is an essential feature of *noninvasive* control technique, common to both OGY-based techniques [1] and all DFC-based methods [3–6].

Let us then consider the following one-dimensional map with an additional variable:

$$x_{n+1} = f(x_n, a) + k_n, \tag{1}$$

$$k_{n+1} = g_n(x_n, k_n), \tag{2}$$

where f represents the original system, n is the time index, $x_n, k_n \in \mathbb{R}$, and a is a control parameter fixed so that the map (1) would produce a chaotic orbit for $k_n \equiv 0$. We assume that the function f is upward single humped. The function g_n is taken as a modification of the feedback adjustment function in Ref. [10]. The mechanism of g_n is schematically illustrated in Fig. 1(a).

Let T and L (the targeting period) be integer parameters. First, one iterates system (1) with a constant value of k_n $(=k_0)$ until $n \geqslant T$. Then one scans the generated time series by T-length time intervals. Here, the locking condition is that the second largest value and the first largest value (denoted by $\hat{x}$) in a T-length scanning time interval be L length away

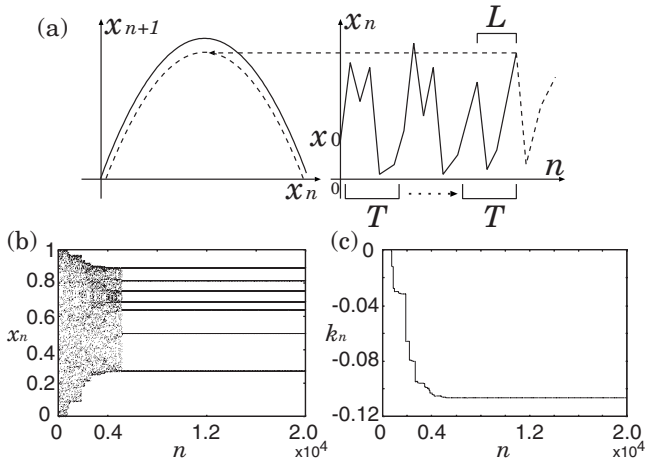

FIG. 1. (a) Schematic illustration of the locking process. The solid map (left) generates the solid time series (right). The dashed map (left) is the adjusted one, when the locking condition holds. (b) Time series of x_n when locking control is applied. (c) Corresponding time series of k_n. $L=7$, $T=24$, $N=20\,000$, and $T'=20\,000$.

from each other in that order. When the locking condition does not hold, the function g_n is defined as $g_n(x_n,k_n)\equiv k_n$ and one continues updating x_n Eqs. (1) and (2). Once the locking condition is met, k_n is adjusted such that $\hat{x}$ is equal to the maximum of $f(x,a)+k_{n+1}$; i.e., the g_n is defined as $g_n(x_n,k_n)\equiv\hat{x}-x_e$, where x_e represents the approximated maximum of the function f. x_e is derived as the largest value of the T'-($\gg T$) length time series obtained in advance from the iterations of Eq. (1) without k_n. Here, T' is a integer parameter which is determined as an appropriate large value so as to approximate the maximum well. After the adjustment of k_n, one iterates Eq. (1) for the adjusted k_n more than T steps and restarts scanning.

The adjustment is done using the approximated maximum of the function $f(x,a)+k$, which is denoted by $h(k)$, where k is an adjustable parameter and $h(k)=x_e+\epsilon k$, with $\epsilon=1$. Notice that the value of ϵ is independent of the function f, and therefore, the method is applicable to generic single-humped maps f. We repeat the locking procedure until $n=N$ for initial conditions x_0 and k_0.

To illustrate that the locking process can work appropriately so as to obtain period-L periodic orbits, we show numerical simulations in the case of the logistic map $f(x,a)=ax(1-x), a=4$. Figures 1(b) and 1(c) show the time series x_n and k_n, respectively, when the locking is applied with $L=7$.

Table I shows the numbers of POs, whose period is related to the value of L, with respect to 5 sorts of L and 128 initial values of x_0. The initial values are chosen in [0,0.5] and $k_0=0$. Here we consider the period of POs to be L when the period is L or a multiple of L. The period is determined to an accuracy of 2^{-7} with negativity of the Lyapunov exponents. The values of T in Table I are determined such that the number of period-L POs becomes maximum in $T<30$. The lowest row of the table shows the numbers of period-L POs obtained by the original method [10] when $T=20$.

The adjustment action towards periodic windows in the CF's parameter space is similar to the original method in Ref. [10]. In the original method, locally stable attractors of the dynamics for k_n exist in periodic windows and k_n is changing its value until trapped in a periodic window and converging to the attractors.

TABLE I. Number of POs whose period is L with respect to 128 initial values of x_0. The lowest row shows the number of period-L POs obtained by the original method [10]—i.e., without locking when $T=20$. $N=20\,000$, and $T'=20\,000$.

L	2	3	5	7	11
T	3	8	16	23	17
Number of POs	109	119	77	56	5
Number of POs (original)	107	49	25	1	0

Moreover, the locking condition limits the adjustment action. Once the orbit is trapped in a periodic window (the period is less than T), the order pattern of the time series in every T-length scanning interval is also changing periodically. Hence, the adjustment action is going to be terminated in the trapping periodic window, especially where the period of the window is L. The period of the obtained PO is nL, where n is a positive integer satisfying the condition $nL<T$.

More precisely, if $1<n$, then the obtained POs correspond to the locally stable attractors encountered in the original method. In this case, k_n converges to such attractors. On the other hand, if $n=1$, then the locking condition terminates the adjustment action completely and thus k_n stops changing its value not exactly at the attractors. This is because the largest and second largest values (L length apart) have coalesced.

The trapping processes of a period-L periodic window are illustrated in Fig. 2. The shaded (green) part represents the regions where the second largest points can exist when the locking condition holds. The upper bound of the shaded regions corresponds to period-L UPOs. As shown in Figs. 2(a) and 2(c), the largest and second largest points move along the period-L UPOs. Therefore, the period of the trapping periodic window is L. In Fig. 2(b), the locally stable attractor for k_n is shown as the intersection between the dash-dotted line $[x=h(k)]$ and the largest points of POs in the periodic window.

It should be noted that the period of the trapping periodic windows is not necessarily related to L, since an infinite number of periodic windows exist and it would happen that the k_n is trapped by non-L periodic windows. Additionally, if the value of k_n goes beyond a critical value, then a boundary crisis occurs. To avoid this, some return process of the excess of k_n to 0 has been discussed [10]. However, for simplicity, we do not consider here such an occurrence of the crisis.

Let us next apply the method to continuous-time systems, such as the Rössler model [13] and the three-dimensional Belouzov-Zhabotinsky (BZ) reaction model [14]. As these systems are highly dissipative, the attractors are stretched in one direction on the Poincaré surface of section, and hence they may be reduced to one-dimensional maps. Thus, we add an impulsive control feedback only to the one system variable on the Poincaré surface of section. Here, the strength of the feedback corresponds to k_n in discrete-time systems. It

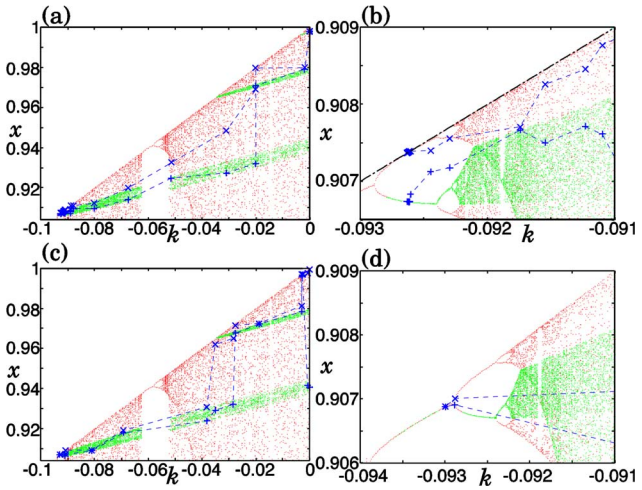

FIG. 2. (Color online) Adjustment processes in the bifurcation diagram with respect to k. The green (shaded) parts represent the regions where the second largest points can exist when the locking condition holds. The $\times$ and $+$ denote the largest and second largest values (L length apart) for each k_n. (a), (b) The case that the period of the obtained PO is $2L$. (b) The enlargement around the trapping periodic window in (a). The dash-dotted line shows $x=h(k)$. (c), (d) The case that the period is L. (d) The enlargement around the trapping periodic window in (c). $L=5$, $T=16$, $N=20\,000$, and $T'=20\,000$.

should be noticed that, in the case of the Rössler model and the BZ reaction model, the minima of the reduced return maps are focused, since the reduced return maps are downward single humped. Hence, in this case, $h(k)$ corresponds to the approximated minimum of the function $f(\cdot)+k$.

A technical remark for the proportionality factor ϵ in $h(k)$ is in order when we apply the method to continuous-time systems. While $\epsilon=1$ holds in the case of discrete-time systems, ϵ is not necessarily 1 in the case of continuous-time systems. This may be because, although we add the impulsive feedback control signal k_n only to one of three system variables, the attractors on the Poincaré surface of section are not completely parallel to the direction of the one controlled variable. The Poincaré surface of section is selected with respect to the minima of the x variable in the Rössler model [13] and minima of the v variable in the BZ reaction model [14]. Here, we approximate the minimum of the reduced return map ($k_n=0$) by the smallest value of the T'-length time series. The slopes of $h(k)$, which should correspond to ϵ, are estimated to be about 1 and 1.87 for the Rössler model and the BZ reaction model, respectively.

Figures 3(a) and 3(b) show the result when the locking method with $L=6$ is applied to the Rössler model by means of the reduced one-dimensional map. Figure 3(a) shows the time series of x_n and k_n. Figure 3(b) shows the controlled period-6 orbit. Figures 3(c) and 3(d) show the application to the BZ reaction model with $L=5$. The controlled period-5 orbit is shown in Fig. 3(d).

III. TRACKING METHOD

As shown in Figs. 3(b) and 3(d), due to the impulsive nature of the feedback considered in the present case, the

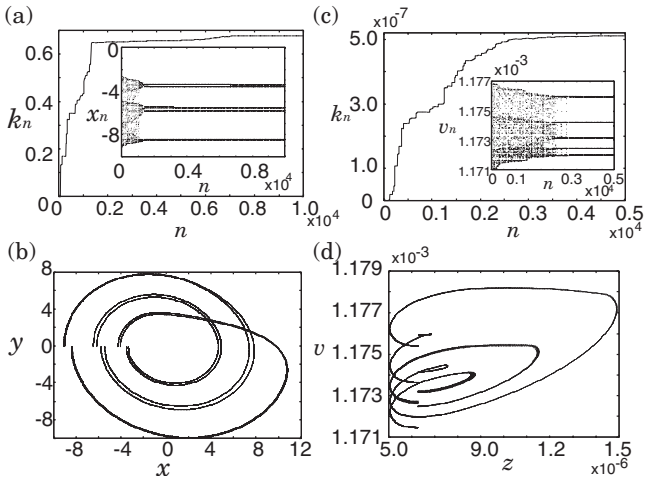

FIG. 3. (a) Time series of k_n (inset: time series of x_n) for the Rössler model. (b) Controlled period-6 orbit. $L=6$, $T=19$, $N=10\,000$, $T'=10\,000$, $k_0=0$, and $\epsilon\simeq 1$. (c) Time series of k_n (inset: time series of x_n) in the BZ reaction model. (d) Controlled period-5 orbit. $L=5$, $T=15$, $N=5000$, $T'=10\,000$, $k_0=0$, and $\epsilon\simeq 1.87$.

controlled POs have discontinuities at the Poincaré surface of sections. Thus, the discontinuous periodic orbits are different from the UPOs embedded within the original chaotic attractor.

To trace back the controlled POs to the original UPOs, an additional step has to be introduced, consisting of a tracking method of periodic orbits that changes the value of k_N ($\equiv K$) slightly in the direction of making it vanish. To save energy consumption for the whole control process, the tracing back of the POs should be necessary with causing the additional parameter K to vanish and recovering the original dynamics.

Let the pre-image of the controlled period-L POs in the reduced one-dimensional map be described as the solution of the following equation:

$$F(x,K) = F^{L+1}(x,K), \tag{3}$$

where $F(x,k)=f(x,a)+k$, and here f represents the reduced maps ($k_n=0$) and hence is downward humped. Let us consider the smallest point of the controlled PO. The pre-image of the smallest point is closest to the critical point in the periodic orbit, which is denoted by X_p.

We track the pre-image by the following procedure (see Fig. 4). First, we change the value of K to K' by ΔK. If $|\Delta K|$

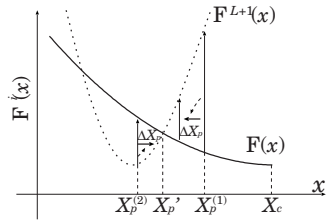

FIG. 4. Schematic illustration for control from X_p to X_p' in the case of a downward-humped map and $X_c > X_p'$. If $X_p^{(1)} > X_p'$, then $\Delta X_p < 0$. If $X_p^{(2)} < X_p'$, then $\Delta X_p > 0$.

is sufficiently small, the pre-image X'_p [the solution of Eq. (3) for K'] is close to X_p. Here, let us describe the solution of Eq. (3) as the x coordinate of the intersection between the curves $y=F(x,K)$ and $y=F^{L+1}(x,K)$ in the (x,y) plane. Then, X'_p is the same position in the two curves $y=F(x,K')$ and $y=F^{L+1}(x,K')$ as is the case of X_p.

In the next step, it is possible to control X_p to X'_p in the following manner. First, we change X_p to $X_p-\Delta X_p$. The ΔX_p is determined as $\Delta X_p=\sigma\,\mathrm{sgn}(X_p-X_c)[F(X_p,K')-F^{L+1}(X_p,K')]$, where σ is a parameter with $0<\sigma\ll 1$. X_c denotes the critical point which is approximated by the pre-image of x_e in the initial T'-length chaotic orbit. It should be noticed that application to continuous-time systems needs further estimation of the location of the critical point X_c with respect to K' as well as ϵ.

The sign of ΔX_p is determined as illustrated in Fig. 4 which shows the case that $X_c>X'_p$. The value of $|F(X_p,K')-F^{L+1}(X_p,K')|$ is decreasing as X_p is approaching X'_p. Thus, X_p is converging to X'_p.

After convergence to X'_p, we change K' by ΔK again and repeat the procedure controlling to X'_p until K vanishes. As a result, the controlled POs converges to the period-L UPOs embedded within the original chaotic attractor. Note that, as shown in Fig. 4, the position of X'_p corresponds to a destabilized node, since the periodic orbit first controlled by the locking adjustment method corresponds to a node appearing by saddle-node bifurcation.

We introduce the above tracking technique as a simple example to track UPOs in one-dimentional unimodal maps. In this technique, the value of ΔK has to be chosen carefully not to displace the position of the targeting UPO. We can also consider another technique [15] for tracking UPOs.

We apply the locking adjustment and the tracking method to the Rössler model and the BZ reaction model by means of the reduced one-dimensional map on the Poincaré section. The tracking processes of $F(X'_p,K')$ with the partial bifurcation diagrams with respect to the controlled variables on the Poincaré sections are shown in Figs. 5(a) and 5(d). Figures 5(b), 5(c), 5(e), and 5(f) show the controlled and tracked UPOs. The discontinuities of the stable POs as shown in Fig. 3 disappear as the values of K vanish.

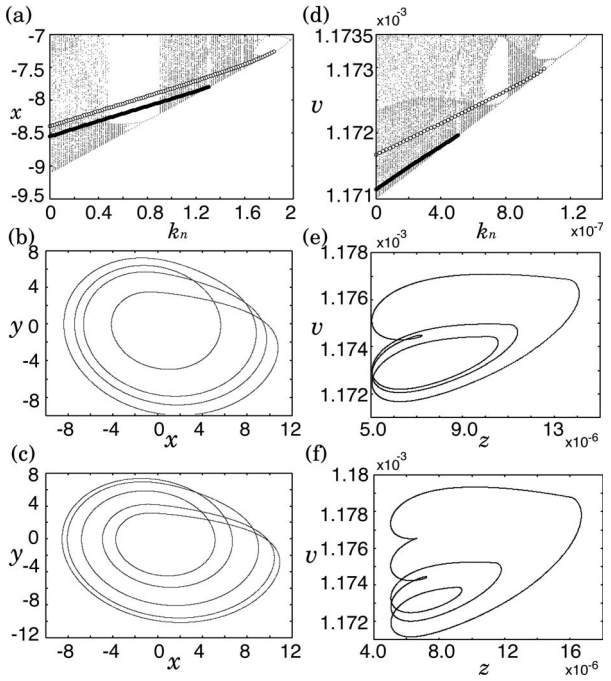

FIG. 5. (a), (b), (c) Tracking process of POs for the Rössler model with the partial bifurcation diagram with respect to x on the section. (a) The circles show the loci of $F(X'_p,K')$. The open and solid circles represent period-4 and period-5 POs, respectively. The controlled and tracked UPOs are shown in (b) period-4 ($T=10$, $L=4$, $k_0=1$) and (c) period-5 ($T=10$, $L=5$, $k_0=1$). $N=7000$, $T'=10\,000$, $\epsilon\simeq 1$, $\sigma=0.05$, and $\Delta K=K/100$. (d), (e), (f) Tracking process of POs for the BZ reaction model. (d) The open and solid circles represent period-4 and period-5 POs, respectively. The UPOs are shown in (e) period-4 ($T=8$, $L=4$) and (f) period-5 ($T=15$, $L=5$). $N=5000$, $T'=10\,000$, $k_0=0$, $\epsilon\simeq 1.87$, $\sigma=0.005$, and $\Delta K=K/50$.

IV. DISCUSSION AND CONCLUSION

Finally, we discuss the robustness of the method against additive noise, as this is a crucial point to be assessed in view of applications to experimental systems. To this purpose, we apply the method to the Rössler system with an additional noise term $D\xi(t)$ in the variable x, where D is a amplitude parameter and $\xi(t)$ is a white noise process with zero mean and δ correlated in time $[\langle\xi(t)\xi(t')\rangle=\delta(t-t')]$.

In Fig. 6 we show an example of the behavior of the Rössler system with noise when the method is applied. Namely, Figure 6(a) shows the results by the time series of x_n and k_n. The controlled and tracked period-3 UPO is shown in Fig. 6(b). The amplitude of the additional noise $D=0.2$ is about 1% of the signal amplitude. Moreover, we also investigate the noise resistance of the method with respect to 100 different initial conditions for the same amplitude of noise and numerically confirm the success of the method in 66 cases.

In conclusion, we presented a robust and reliable method to control a chaotic orbit into a UPO which has the desired period. The method does not require any detailed information of the controlled system such as system parameters, but

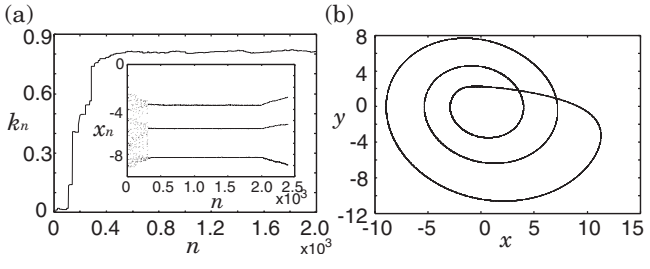

FIG. 6. Control and tracking process in the Rössler system with noise. $D=0.2$. (a) Time series of k_n (inset: time series of x_n including tracking process). (b) Controlled and tracked period-3 UPO. $T=10$, $L=3$, $k_0=0$, $N=2000$, $T'=200$, $\epsilon=1$, $\sigma=0.05$, and $\Delta K=K/100$.

uses automatically adjusting feedback of the additional parameter. Moreover, the method also uses a tracking technique by means of the intersections of multiple one-dimensional return maps. The control has been achieved without reference states for targeting POs, given only integers which correspond to the periods. The method does not require a reconstruction of the parametrical variations in the UPOs' stable and unstable manifolds, nor pretuning of the principal parameters, and therefore it provides an appropriate strategy to control fast dynamical processes in real time toward desirable periodic dynamics.

The authors gratefully thank Professor K. Showalter and Professor M. Herrmann for their valuable suggestions. This work is partially supported by Superrobust Computation Project in 21st Century COE Program on Information Science and Technology Strategic Core from the Ministry of Education, Culture, Sports, Science, and Technology, the Japanese Government.

[1] E. Ott, C. Grebogi, and J. A. Yorke, Phys. Rev. Lett. **64**, 1196 (1990).
[2] S. Boccaletti, C. Grebogi, Y.-C. Lai, H. Mamcini, and D. Maza, Phys. Rep. **329**, 103 (2000).
[3] K. Pyragas, Phys. Lett. A **170**, 421 (1992).
[4] J. E. S. Socolar, D. W. Sukow, and D. J. Gauthier, Phys. Rev. E **50**, 3245 (1994).
[5] A. Ahlborn and U. Parlitz, Phys. Rev. Lett. **93**, 264101 (2004).
[6] A. Ahlborn and U. Parlitz, Phys. Rev. Lett. **96**, 034102 (2006).
[7] S. Parthasarathy and S. Sinha, Phys. Rev. E **51**, 6239 (1995).
[8] N. Parekh, S. Parthasarathy, and S. Sinha, Phys. Rev. Lett. **81**, 1401 (1998).
[9] R. V. Sole, J. G. P. Gamarra, M. Ginovart, and D. Lopez, Bull. Math. Biol. **61**, 1187 (1999).
[10] H. Ando and K. Aihara, Phys. Rev. E **74**, 066205 (2006).
[11] D. Huang, Phys. Rev. Lett. **93**, 214101 (2004).
[12] D. Huang, Phys. Rev. E **73**, 066204 (2006).
[13] O. E. Rössler, Phys. Lett. **57**, 397 (1976).
[14] L. Györgi and R. J. Field, Nature (London) **355**, 808 (1992).
[15] V. Petrov, M. J. Crowley, and K. Showalter, Phys. Rev. Lett. **72**, 2955 (1994).